

Dynamic Coupling Phenomena in Molecular Excited States. II. Autoionization and Predissociation in H₂, Hd, and D₂

R. Stephen Berry

Department of Chemistry and The James Franck Institute, University of Chicago, Chicago, Illinois 60637

and

Svend Erik Nielsen

Chemistry Laboratory III, H. C. Ørsted Institute, University of Copenhagen, Copenhagen 2100, Denmark

(Received 4 August 1969)

Vibrationally induced autoionization and one class of predissociation of electronically excited H₂ and its isotopes are treated by a perturbed-stationary-state theory. Autoionization and predissociation rates are given for a number of states of H₂, HD, and D₂. In addition to direct bound-continuum coupling, consideration is given to effects of higher-order coupling; these effects cause order-of-magnitude changes in isolated cases. The auto-ionization rates vary with principal quantum number n as n^{-3} , directly with vibrational energy vhv , and decrease sharply with vibrational quantum change Δv . As the principal quantum number increases, transitions of successively smaller Δv become possible; the net effect of this is to override the n^{-3} dependence in total autoionization rates. Competition between predissociation and autoionization is examined; the two processes show very different dependence on n and v , with the consequence that decay in most regions of (n, v) space is dominated by one or the other process; but the two mechanisms are competitive for some (n, v) states. The isotope effect also is rather different for the two decay processes, enough so that, in effect, the isotope effect amounts to a qualitative change from one mechanism of decay to the other, with mass change.

I. INTRODUCTION

In the preceding paper,¹ we describe the general method we have used to analyze the vibrational-electronic coupling phenomena in H₂. Our aim is to use H₂ as a model system to study the microscopic origins of the various processes, including vibronic perturbations in Rydberg states, autoionization, predissociation, associative ionization, and dissociative recombination. The method, utilizing stationary-state basis functions for the complete particle system in the Born-Oppenheimer approximation, puts all the processes on the same footing and enables us to compare competing processes and to treat coupling processes beyond the simplest first-order processes.

In principle, one might expect all possible channels to interact when one has a system consisting of 2 electrons, 2 protons, and some 13 eV of energy. The actual situation for H₂ is not as complex as it might be. The principal channels for associative ionization, dissociative recombination, and collisional ionization are all virtually uncoupled from autoionization, predissociation, and vibronic coupling among Rydberg states. These last three phenomena are rather interwoven. It is the purpose of this paper to examine autoionization in particular, and, in a somewhat narrower way, predissociation and vibronic coupling. Our treatment of these phenomena has been restricted to the $np\sigma$ and $np\pi$

states, which are optically accessible from the molecular ground electronic state. A preliminary report has been given describing some of the calculations included in this discussion.²

II. AUTOIONIZATION

The photoionization of H₂ in the region 0–2 or 3 eV above threshold is now known to be due principally to autoionization. The high-resolution experiments of Berkowitz and Chupka^{3,4} and of Comes and Wellern⁵ show unambiguously that the total photoionization current of H₂⁺ produced by photons in this energy range consists of a small contribution from the continuous background of direct transitions to the continuum and a very large contribution from rather sharp peaks. The high-resolution experiments have shown that the peaks can be associated with specific rotational and vibrational levels of known Rydberg states of H₂; presumably these Rydberg states are the long-lived intermediate states from which autoionization occurs. The experiments indicate that, in the region near threshold, the overwhelming part of the dipole oscillator strength and, more specifically, of the total photoionization cross section is due to transitions to these Rydberg states rather than to the continuum.

Our task consists of several steps. The calculation of transition probabilities to the Rydberg and continuum states is one of these, but has not yet

been studied. The other steps all deal with the mechanism of the coupling process and its consequences. The mechanism that has seemed most reasonable for autoionization of H_2 (but not necessarily of larger molecules) is coupling of electronic states by the nuclear kinetic-energy operator, i. e., the breakdown of the Born-Oppenheimer approximation,^{2, 6-8} or vibronic coupling, as this process is also called. We must be very careful to recognize that in many other molecular examples, as well as in atoms, the mechanism for autoionization is likely to be best represented as configuration interaction. Specifically, this mechanism, the most obvious and probable alternative to vibrationally induced coupling, is due to electron correlation. The corresponding operator may be represented as $\sum_i \langle j | r_{ij}^{-1} | i \rangle$, or better, as the electronic fluctuation potential – the difference between $\sum r_{ij}^{-1}$ and the Hartree-Fock effective potential.

The vibronic mechanism carries with it several implications that can be used directly without recourse to microscopic calculations. First, because of their relative time scales, rotation (for states of low J) is much less effective than vibration as a device to break down the stationary character of the Rydberg states. Second, as Bardsley⁷ has pointed out, the autoionization rates should vary as n^{-3} , where n is the principal quantum number of Rydberg states; this inference is due to the scale factor for the inner part of the Rydberg orbital. Third, the autoionization rates depend very sensitively on Δv , the change of vibrational quantum number of the core, because the effect of the coupling operator is primarily that of the nuclear momentum operator acting on a slightly anharmonic oscillator function. This gives us the propensity rule for probabilities:

$$\text{prob}(\Delta v = -1) \gg \text{prob}(\Delta v = -2) \gg \dots$$

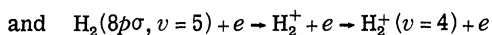
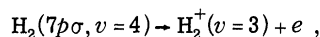
Actually this rule is only valid when the initial and final vibrational states differ by no more than about three or four vibrational quanta. For differences of four or five quanta or more, the transition amplitudes, all very small, depend in a very sensitive way on the details of the potential curves. The nonzero part of the transition amplitudes in such cases can be thought of as the accidental residues due to imperfect cancellation of large and almost equal positive and negative contributions.

Fourth, a kind of dependence that has perhaps been given less emphasis than the others is the dependence on vibrational quantum number or vibrational energy. The matrix elements of the momentum operator for the harmonic oscillator depend on $(\omega v)^{1/2}$, for $(v | p | v - 1)$, and on $[\omega(v + 1)]^{1/2}$, for $(v | p | v + 1)$, so that we expect the autoionization rates to depend on the vibrational

energy of the Rydberg state.

The calculations based on our model for $H_2^+ + e$ bear out these implications from the simpler analysis, provided the vibrationally induced process dominates the autoionization. Experimental evidence from the linewidth measurements of Chupka and Berkowitz⁴ now gives a strong indication that this is so. The experimental rates based on peak shapes (with apparatus widths deconvoluted) do decrease with increasing n , increase with increasing v , and in most cases decrease with increasing Δv . However, most lines corresponding to transitions with $|\Delta v| > 1$ had widths corresponding to the apparatus resolution. The correlation of the values of theoretical and experimental rates is quite good; the values differ at worst by a factor of 5 and in most cases differ by factors of 2 or 3. Experimental values are systematically higher than theoretical values.

A number of calculated autoionization rates are given in Tables I–III for H_2 , HD, and D_2 . These rates are based on the assumption of first-order coupling only, so that the coupling rate is given by the Wentzel-Fermi golden-rule rate $= (2\pi/\hbar) \times |T_1|^2 \rho$, where ρ is the density of final states. Figure 1 shows the theoretical autoionization rates for $np\sigma$ and $n\pi$ states of H_2 as functions of the state energies. Rates for other states can be calculated for states of higher n by means of the n^{-3} scaling law. Thus, although the transitions



are all energetically forbidden for the system described by our model Hamiltonian, we may estimate the rates of these processes for real H_2 from the theoretical rates for autoionization of $H_2(9p\sigma, v=4, 5)$. We obtain 1.73×10^{12} , 1.16×10^{12} , and $1.59 \times 10^{12} \text{ sec}^{-1}$ for the three one-quantum processes this way. The $\Delta v = -2$ processes energetically allowed by the model Hamiltonian are 8.7×10^9 , 5.7×10^9 , and $1.3 \times 10^{10} \text{ sec}^{-1}$, respectively, while the experimentally determined values are 9.0×10^{11} , 8.0×10^{12} (with uncertain identification), and $2 \times 10^{12} \text{ sec}^{-1}$. The dependence of autoionization rates on Δv obeys the propensity rule so long as the states, initial and final, can be regarded as two states of a nearly harmonic oscillator. As the tables show, we find that for autoionization processes having large Δv 's and very slow rates, the vibrational propensity rule is not obeyed. In practice, this breakdown occurs for $\Delta v \geq 5$ and for rates less than 10^9 sec^{-1} . The practical consequence of the breakdown is that for such slow processes the rate is a very sensitive function of the potentials of the two states.

The details of the coupling mechanism can be summarized as follows: The "first derivative"

TABLE I. Autoionization rates (sec^{-1}) of $np\sigma$ and $np\pi$ Rydberg states of H_2 , for various initial and final vibrational quantum numbers v_i and v_f and core rotational quantum numbers K . Powers of 10 are indicated in parentheses. Closed channels are denoted by "x," experimental values from Ref. 4 are in square brackets beneath the theoretical values.

A. $np\sigma$ states		n	K	4	5	6	7	8	9	10
v_i	v_f									
1	0	0	0	x	x	x	x	2.1(11) [4.0(11)]	1.5(11) [3.0(11)]	1.1(11)
		1	1	x	x	x	x	2.2(11)	1.5(11)	1.1(11)
		3	3	x	x	x	x	2.2(11)	1.5(11)	1.1(11)
2	0	0	0	x	x	1.5(9)	9.5(8)	6.4(8)	4.6(8)	3.3(8)
		3	3	x	x	1.6(9)	1.0(9)	7.1(8)	5.1(8)	3.7(8)
2	1	0	0	x	x	x	x	4.7(11) [1.3(12)]	3.2(11)	2.3(11)
		3	3	x	x	x	x	4.8(11)	3.3(11)	2.3(11)
3	0	0	0	x	x	1.7(6)	9.4(5)	5.9(5)	3.9(5)	2.8(5)
3	1	0	0	x	x	5.1(9)	3.3(9)	2.2(9)	1.6(9)	1.15(9)
3	2	0	0	x	x	x	x	7.9(11) [2.7(12)]	5.4(11)	3.9(11)
4	0	0	0	x	7.4(6)	4.5(6)	2.9(6)	2.0(6)	1.4(6)	1.0(6)
4	1	0	0	x	2.4(7)	1.6(7)	1.1(7)	8.1(6)	5.8(6)	4.3(6)
4	2	0	0	x	x	1.3(10)	8.7(9)	5.8(9)	4.1(9)	3.0(9)
4	3	0	0	x	x	x	1.7(12) ^a	1.1(12) ^a	8.1(11)	5.8(11)
5	0	0	0	1.1(8)	5.5(7)	3.2(7)	[9.0(11)]	[8.0(12)]	[2.7(12)]	[2.0(12)]
5	2	0	0	x	1.9(8)	1.2(8)	2.0(7)	1.3(7)	9.2(6)	6.7(6)
5	3	0	0	x	x	3.1(10)	8.4(7)	5.9(7)	4.2(7)	3.1(7)
5	4	0	0	x	x	x	2.0(10)	1.3(10)	9.3(9)	6.8(9)
							x	1.6(12) ^a	1.1(12)	8.0(11)
6	4	0	0	x	x	x	4.0(10)	[2.0(12)]	[5.8(12)]	[1.7(12)]
6	5	0	0	x	x	x	x	2.7(10)	1.9(10)	1.4(10)
								x	1.5(12)	8.0(11)

TABLE I. (continued).

B. $np\pi$ states		4	5	6	7	8	9	10
v_i	v_f	n						
1	0	0	x	x	x	1.9(11) [3.0(11)]	1.4(11)	1.0(11)
2	0	0	x	1.3(9)	8.7(8)	6.1(8)	4.4(8)	3.2(8)
2	1	0	x	x	x	4.2(11)	3.0(11)	2.2(11)
3	0	0	x	3.2(6)	8.8(5)	[9.0(11)]		
3	1	0	x	x	3.0(9)	2.1(9)	1.5(9)	1.1(9)
3	2	0	x	4.4(9)	x	7.0(11)	4.95(11)	3.6(11)
4	0	0	1.1(7)	6.6(6)		[2.0(12)] ^b		
4	1	0	x	2.1(7)	1.5(7)	5.5(9)	4.0(9)	2.9(9)
4	2	0	x	x	1.2(10)	1.0(12)	7.4(11)	5.4(11)
4	3	0	x	x	x	x	x	x
5	0	0	9.2(7)	5.0(7)	2.8(7)	1.8(7)	9.0(6)	6.6(6)
5	1	0	2.6(6)	1.5(6)	9.5(5)	6.3(5)	3.0(5)	2.3(5)
5	2	0	x	1.6(8)	1.2(8)	7.9(7)	4.0(7)	3.0(7)
5	3	0	x	x	2.6(10)	1.7(10)	8.8(9)	6.5(9)
5	3	3	x	x	2.8(10)	1.2(10)	9.4(9)	7.0(9)
5	4	0	x	x	x	1.3(10)	1.0(12)	7.4(11)
6	1	0	1.7(8)	9.2(7)	5.4(7)	x	1.6(7)	1.2(7)
6	3	0	x	3.8(8)	2.7(8)	1.3(8)	9.7(7)	7.2(7)
6	4	0	x	x	5.4(10)	2.5(10)	1.8(10)	1.3(10)
6	5	0	x	x	x	x	1.3(12)	9.7(11)

^aThese channels are actually closed in our model; their rates have been calculated from the scaling law.

^bNo assignment was given in Ref. 4 for the line at 775.12 Å; this is merely our presumption.

TABLE II. Autoionization rates (sec^{-1}) for specific vibrational states of Rydberg series of HD. (All states taken with $K=0$.)

A. $np\sigma$ states		n	K	4	5	6	7	8	9	10
v_i	v_f									
1	0			x	x	x	x	1.8(11)	1.2(11)	9.0(10)
2	0			x	x	1.0(9)	6.9(8)	4.7(8)	3.3(8)	2.4(8)
2	1			x	x	x	x	x	2.7(11)	1.9(11)
3	0			x	3.8(6)	1.8(6)	1.0(6)	6.6(5)	4.5(5)	3.2(5)
3	1			x	x	3.6(9)	2.3(9)	1.6(9)	1.1(9)	8.2(8)
3	2			x	x	x	x	x	4.5(11)	3.2(11)
4	0			x	2.6(7)	1.5(7)	9.5(6)	6.4(6)	4.5(6)	3.2(6)
4	1			x	x	6.5(6)	4.6(6)	3.2(6)	2.4(6)	1.8(6)
4	2			x	x	x	5.7(9)	3.9(9)	2.7(9)	2.0(9)
4	3			x	x	x	x	x	6.7(11)	4.8(11)
5	0			6.2(7)	3.0(7)	1.7(7)	1.1(7)	7.2(6)	5.0(6)	3.6(6)
5	1			x	2.3(7)	1.3(7)	8.1(6)	5.4(6)	3.8(6)	2.8(6)
5	2			x	x	7.7(7)	5.1(7)	3.6(7)	2.5(7)	1.9(7)
5	3			x	x	x	1.2(10)	8.2(9)	5.8(9)	4.2(9)
5	4			x	x	x	x	x	9.2(11)	6.5(11)
B. $np\pi$ states										
1	0			x	x	x	x	1.6(11)	1.1(11)	8.4(10)
2	0			x	x	9.3(8)	6.3(8)	4.4(8)	3.2(8)	2.4(8)
2	1			x	x	x	x	3.4(11)	2.5(11)	1.8(11)
3	0			x	3.1(6)	1.6(6)	9.7(5)	6.3(5)	4.3(5)	3.1(5)
3	1			x	x	3.1(9)	2.1(9)	1.5(9)	1.1(9)	7.9(8)
3	2			x	x	x	x	x	4.1(11)	3.0(11)
4	0			x	2.3(7)	1.4(7)	9.0(6)	6.1(6)	4.4(6)	3.2(6)
4	1			x	7.6(6)	5.9(6)	4.3(6)	3.1(6)	2.3(6)	1.7(6)
4	2			x	x	7.5(9)	5.1(9)	3.6(9)	2.6(9)	1.9(9)
4	3			x	x	x	x	x	6.0(11)	4.4(11)
5	0			4.9(7)	2.7(7)	1.6(7)	1.0(7)	6.9(6)	4.9(6)	3.6(6)
5	1			x	2.0(7)	1.2(7)	7.7(6)	5.2(6)	3.7(6)	2.7(6)
5	2			x	9.8(7)	6.9(7)	4.8(7)	3.4(7)	2.5(7)	1.8(7)
5	3			x	x	x	1.1(10)	7.6(9)	5.5(9)	4.1(9)
5	4			x	x	x	x	x	8.2(11)	6.0(11)

TABLE III. Autoionization rates (sec^{-1}) for specific vibration-rotation rates of Rydberg series of D_2 . (All states taken with $K=0$.)

A. $np\sigma$ states											
v_i	v_f	n	4	5	6	7	8	9	10		
1	0		x	x	x	x	x	1.0(11)	7.2(10)		
2	0		x	x	x	4.7(8)	3.2(8)	2.3(8)	1.7(8)		
2	1		x	x	x	x	x	2.2(11)	1.5(11)		
3	0		x	x	7.4(6)	4.4(6)	2.9(6)	2.0(6)	1.4(6)		
3	1		x	x	x	1.4(9)	9.4(8)	6.7(8)	4.9(8)		
3	2		x	x	x	x	x	x	2.5(11)		
4	0		x	3.4(7)	1.9(7)	1.2(7)	8.0(6)	5.6(6)	4.1(6)		
4	1		x	x	1.9(5)	1.9(5)	1.6(5)	1.3(5)	1.0(5)		
4	2		x	x	x	3.4(9)	2.3(9)	1.6(9)	1.2(9)		
4	3		x	x	x	x	x	x	3.6(11)		
5	1		x	2.0(7)	1.1(7)	7.2(6)	4.8(6)	3.4(6)	2.4(6)		
5	2		x	x	2.2(7)	1.5(7)	1.1(7)	7.7(6)	5.7(6)		
5	3		x	x	x	6.7(9)	4.5(9)	3.2(9)	2.3(9)		
5	4		x	x	x	x	x	x	4.9(11)		
6	0		1.0(5)	5.3(4)	3.1(4)	1.9(4)	1.3(4)	9.1(3)	6.6(3)		
6	2		x	6.1(7)	1.8(7)	1.1(7)	7.2(6)	5.0(6)	3.6(6)		
6	3		x	x	5.1(7)	3.6(7)	2.5(7)	1.8(7)	1.4(7)		
6	4		x	x	x	1.2(10)	8.1(9)	5.7(9)	4.1(9)		
6	5		x	x	x	x	x	x	6.4(11)		
B. $np\pi$ states											
1	0		x	x	x	x	x	9.0(10)	6.6(10)		
2	0		x	x	x	4.2(8)	3.0(8)	2.1(8)	1.6(8)		
2	1		x	x	x	x	x	1.9(11)	1.4(11)		
3	0		x	x	6.4(6)	4.0(6)	2.7(6)	1.9(6)	1.4(6)		
3	1		x	x	x	1.2(9)	8.7(8)	6.3(8)	4.7(8)		
3	2		x	x	x	x	x	3.1(11)	2.3(11)		
4	0		x	2.8(7)	1.7(7)	1.1(7)	8.7(6)	5.4(6)	4.0(6)		
4	1		x	x	1.8(5)	1.8(5)	1.5(5)	1.2(5)	9.8(4)		
4	2		x	x	x	3.0(9)	2.1(9)	1.5(9)	1.1(9)		
4	3		x	x	x	x	x	x	3.3(11)		
5	1		x	1.7(7)	1.0(7)	6.7(6)	4.6(6)	3.3(6)	2.4(6)		
5	2		x	x	2.0(7)	1.4(7)	1.0(7)	7.4(6)	5.5(6)		
5	3		x	x	x	5.9(9)	4.2(9)	3.0(9)	2.2(9)		
5	4		x	x	x	x	x	x	4.5(11)		

TABLE III. (continued).

v_i	v_f	n	4	5	6	7	8	9	10
6	0		8.2(4)	4.7(4)	2.9(4)	1.9(4)	1.3(4)	8.9(3)	6.6(3)
6	2		x	2.6(7)	1.6(7)	1.0(7)	6.9(6)	4.8(6)	3.5(6)
6	3		x	x	4.5(7)	3.3(7)	2.4(7)	1.8(7)	1.3(7)
6	4		x	x	x	1.0(10)	7.4(9)	5.3(9)	4.0(9)
6	5		x	x	x	x	x	x	5.8(11)

term¹

$$T_1 = \left(\psi_f \chi_f \left| \frac{\partial \psi_i}{\partial R} \right| \partial \chi_i \right) \quad (1)$$

is more important for H₂ than is the term

$$T_2 = \left(\psi_f \chi_f \left| \frac{\partial^2 \psi_i}{\partial R^2} \right| \chi_i \right). \quad (2)$$

(We let Ψ = electronic function and χ = vibrational function; f and i indicate final and initial states.) The term T_2 contributes only a few percent at most, and can be neglected in calculations of the sort described here.

It is convenient to transform T_1 into the form

$$T_1 = \left(\chi_f \left| F(nlm; k\lambda\mu; R) \frac{\partial}{\partial R} \right| \chi_i \right), \quad (3)$$

where

$$F(nlm; k\lambda\mu; R) = (\epsilon_{nlm} - \epsilon_{k\lambda\mu})^{-1} \\ \times \int \psi_{k\lambda\mu}^*(r, R) \frac{\partial \mathcal{V}}{\partial R}(r, R) \psi_{nlm}(r, R) dr.$$

Here ϵ_j is the electronic energy for the state j ; n, l , and m are the principal (approximate) angular momentum and axial angular momentum component quantum numbers of the bound Rydberg orbital; k, λ , and μ are the momentum and angular momentum quantum numbers of the free electronic state, and $\mathcal{V}(r, R)$ is the effective potential felt by the Rydberg electron. If \mathcal{V} is expanded in spherical harmonics, we find that the dominant part of T_1 comes from the spherically symmetric part of \mathcal{V} , i. e., the *monopole* contribution. The dipole term vanishes for H₂ and D₂ and is negligible for HD. The quadrupole part plays only a small part in autoionization, normally contributing only a few percent to the rate. This is reflected in the low values of autoionization rates computed previously by one of us⁶ and by Russek, Patterson, and Becker,⁸ from a model based on the quadrupole term only. (The quadrupole term does contribute a large part of the cross section for associative ionization in a few specific cases, particularly of $nd\sigma$ states. This point will be discussed in a subsequent paper dealing with associative ionization and dissociative recombination.) The importance of the monopole term does not lie solely with its influence on rates. The existence of this term makes possible transitions in which the H₂⁺ core is in its rotationless ($K=0$) state, initially and finally. Were the quadrupole (or dipole) term the lowest nonvanishing contribution, $K=0 \rightarrow K=0$ would be strictly forbidden. The dominance of the monopole term means that, in fact, $K=0 \rightarrow K=0$ autoionizing transitions are as probable as are any other allowed transition. Thus, in the P branches of transitions through $np\sigma$ states in cold orthohydrogen,

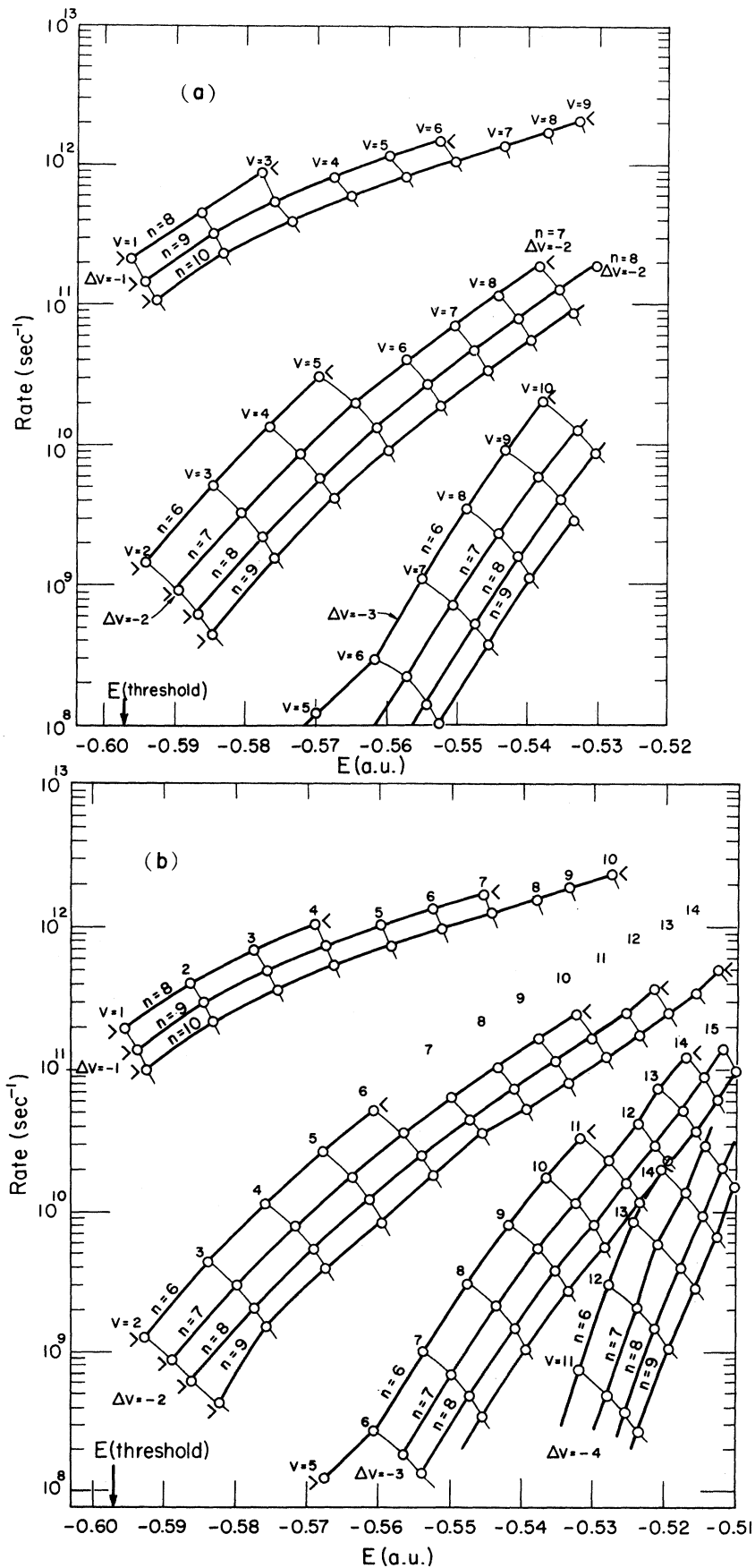


FIG. 1. Autoionization rates for Rydberg states of H_2 , as functions of the energy E , principal quantum number n , and vibrational quantum number v of the initially excited Rydberg state; and of the change Δv in the vibrational quantum number of the core. The value -0.5 a.u. corresponds to $H^+ + H(1s) + e$ at infinite separation and with no kinetic energy. (1 a.u. = 27.21 eV) (a) $np\sigma$ states; (b) $np\pi$ states. First and last states for which a particular decay channel is open, within our model, are indicated by ">" and "<". Note particularly the clustering of curves for various n and a fixed Δv , and the increasing slope of these curves (albeit decreasing rates) with increasing Δv . All states have core rotational quantum number $K=0$.

we expect to see autoionization rates similar to those in the $np\sigma$ states arising from cold parahydrogen. Similarly, the R -branch $np\pi$ states from cold parahydrogen are also capable of rapid autoionization, as the data of Chupka and Berkowitz⁴ show.

The first paper in this series dealt with perturbations among Rydberg states.¹ The vast differences in autoionization rates shown in Tables I–III, and the possibility of mixing among the Rydberg states, together imply that one must consider coupling beyond first order. A Rydberg state Ψ_1 may couple only very weakly with the continuum for autoionization Ψ_{auto} , but may couple strongly with another Rydberg state Ψ_2 , which itself autoionizes very rapidly. This phenomenon does indeed occur and is quite reminiscent of intensity-stealing, as the means by which forbidden optical transitions acquire finite intensities from allowed transitions. In the spectroscopic example, one usually invokes the electric dipole operator for the optical transition and some other operator, such as nuclear kinetic energy or spin-orbit coupling, to accomplish the mixing responsible for the intensity-stealing. In the present case, we may use nuclear kinetic energy as the sole perturbation.

As in the treatment of vibronic coupling among bound Rydberg states, the precise details of higher-order coupling in autoionization depend rather sensitively on the specific potentials and energy levels. In light of this, we can expect the model at hand to provide a qualitative guide of roughly which electronic, vibrational, and rotational states may be expected to show effects of high-order coupling, and to give us an idea of the magnitudes of the coupling. We cannot expect to make statements, at this stage, about specific rotation-vibration levels in the real H_2 molecule. It is better at this point to look for effects of high-order coupling in the form of anomalously large linewidths in the H_2 spectrum. We have previously indicated the region of values of principal quantum number n and vibrational quantum number v , for which high-order vibronic coupling is found in the model. Table IV gives some typical examples of effects of high-order coupling in autoionization.

III. PREDISSOCIATION

The problem of predissociation (and inverse predissociation) is formally very close to that of molecular autoionization. The most probable coupling operators, for molecules in general, must again be the nuclear kinetic energy and the electron-electron correlation. The initial states, as in the case of autoionization, are appropriately represented as products of bound electronic and bound vibrational states. Predissociation differs from autoionization only in that, for predissociation, the final nuclear (radial or vibrational) wave function is a continuum function, and the final electronic function is

bound.

Our work up to this point has dealt only with one class of predissociations. We have examined only the transitions from high vibrational levels of various Rydberg $np\sigma$ and $np\pi$ states into the dissociation continuum of *attractive* Rydberg states of lower principal quantum number, with products $\text{H}(1s) + \text{H}(nl, n \geq 3)$. We have not yet treated transitions into repulsive states such as the $b^3\Sigma_u^+$, or even the predissociation into attractive states such as the $B^1\Sigma_u^+$, dissociating to $\text{H}(n=1) + \text{H}(n=2)$. We have, therefore, omitted some of the probable candidates for known predissociation processes in H_2 . The cases we have treated include a large number of states and are not terribly sensitive to the details of the model. The cases we have neglected seem at this point to be relatively model sensitive and to involve rather specific and perhaps isolated states; for this reason we felt that it was judicious to reserve this latter group for a later and more accurate treatment.

The most important exit channels for predissociation of H_2^* to states with attractive potentials are the channels to $\text{H}(n=1) + \text{H}(n=3)$. This is the result of two physical considerations. First, predissociation rates are very sensitive to the change of nuclear momentum; the smaller the required momentum change, in some average sense, the faster the predissociation rate. This factor tends to inhibit predissociation to attractive states that have $\text{H}(1s) + \text{H}(2s, 2p)$ as their dissociation limit. Secondly, obviously predissociation can only occur from vibrational states (in any specific angular momentum state) which lie above the dissociation limit of the final state. Because the Rydberg levels cluster together as n increases, the number of vibrational states for which predissociation is possible (for normally accessible K values) is extremely limited for those dissociating Rydberg channels giving one atom with quantum number $n \geq 4$. In our model, for $K=0$, for example, the only states of the $7p\sigma$ Rydberg state that may predissociate to the continuum of the $6p\sigma$, to give $\text{H}(n=1) + \text{H}(n=4)$, are those with $v \geq 13$. The rates for such states may be approximated from the n^{-3} scaling law, from the rates given here for predissociation to $\text{H}(n=1) + \text{H}(n=3)$. This scaling is not exact because of the differences in nuclear wave functions, but is quite consistent with the sort of accuracy we may expect of our model.

Rates of predissociation to specific final states from specific Rydberg vibronic states are given in Table V and are shown graphically in Fig. 2. At their fastest, the rates of predissociation are nearly 10^{13} sec^{-1} , significantly faster than autoionization. The rates are relatively independent of the vibrational quantum number in the initial excited state, but depend rather sensitively on the initial and final principal quantum numbers. These two types of dependence reflect the effects of similarity of nu-

TABLE IV. Examples of high-order coupling on autoionization and predissociation rates in H_2 (rates in sec^{-1}).

n	v	Zero-order rate	Rate after coupling	Principal contributing state(s): n	v
A. Autoionization of $n p \sigma$ states					
4	6	2.1 (8)	4.3 (8)	6	3
5	4	2.4 (7)	6.9 (8)	6	3
6	3	5.1 (9)	4.2 (9)		
5	5	1.9 (8)	9.8 (10)	8	3
6	4	1.3 (10)	5.1 (10)	8	3
8	3	7.9 (11)	6.6 (11)		
5	6	3.2 (6)	3.7 (9)	6	5
6	5	3.1 (10)	2.2 (10)		
6	9	9.3 (9)	2.0 (10)	7	8
7	8	1.2 (11)	1.1 (11)	6	9
B. Predissociation of $n p \sigma$ states					
6	9	6.2 (12)	5.7 (12)	7	8
7	8	6.2 (11)	1.2 (12)	6	9
C. Autoionization of $n p \sigma$ states					
5	5	1.6 (8)	1.3 (9)	6	4
6	4	1.2 (10)	2.1 (11)		
9	3	4.9 (11)	3.6 (11)		
4	8	1.3 (7)	1.5 (10)	9	4
5	6	3.8 (8)	1.5 (11)	9	4
6	5	2.6 (10)	3.1 (10)	9	4
9	4	7.4 (11)	5.6 (11)		
5	10	9.4 (7)	1.5 (10)	7	8
7	8	1.1 (11)	8.9 (10)	5	10
D. Predissociation of $n p \pi$ states					
5	10	2.8 (12)	2.5 (12)	7	8
7	8	7.4 (8)	4.1 (11)	5	10

TABLE V. Rates of predissociation (sec^{-1}) of H_2 , HD, and D_2 for states of $K=0$.

n_i	v_i	7	8	9	10	11	12	13	14
A. H_2 $n\rho\sigma$ to $5\rho\pi$									
6	x	6.2(12)	6.4(12)	6.2(12)	5.6(12)	5.3(12)	5.0(12)	4.9(12)	3.8(12)
7	x	6.2(11)	6.2(11)	6.3(11)	6.6(11)	6.2(11)	5.3(11)	5.6(11)	5.3(11)
8	6.6(10)	8.7(10)	8.7(10)	9.6(10)	1.1(11)	1.1(11)	9.8(10)	6.8(10)	7.1(10)
9	1.8(10)	1.9(10)	1.9(10)	2.3(10)	2.4(10)	2.5(10)	2.7(10)	1.7(10)	1.3(10)
10	6.0(9)	5.3(9)	5.8(9)	7.0(9)	6.5(9)	7.5(9)	9.5(9)	6.8(9)	3.4(9)
$n\rho\pi$ to $4\rho\pi$									
5	x	x	2.8(12)	2.8(12)	2.8(12)	2.7(12)	2.6(12)	2.9(12)	2.5(12)
6	x	1.5(10)	1.4(10)	1.8(10)	2.2(10)	2.2(10)	2.1(10)	5.8(9)	6.9(9)
7	x	5.2(8)	7.4(8)	4.5(8)	1.2(6)	8.2(7)	7.7(8)	9.9(8)	2.1(8)
8	3.2(8)	4.1(8)	4.5(8)	6.4(7)	6.4(6)	1.6(7)	3.7(6)	6.2(8)	7.1(7)
$n\rho\pi$ to $3\rho\pi$									
4	x	x	x	x	x	3.1(9)	7.8(8)	5.0(9)	9.2(9)
5	x	x	3.0(8)	7.5(8)	1.1(9)	3.0(8)	4.0(6)	1.1(9)	9.5(7)
B. HD									
$n\rho\sigma$ to $5\rho\sigma$									
6	x	x	x	3.7(12)	3.7(12)	3.6(12)	3.4(12)		
7	x	x	2.0(11)	2.1(11)	2.3(11)	2.3(11)	2.5(11)		
8	1.7(10)	1.9(10)	1.9(10)	1.9(10)	1.9(10)	2.2(10)	2.6(10)		
$n\rho\pi$ to $4\rho\pi$									
5	x	x	x	x	1.0(12)	1.0(12)	1.0(12)		
6	x	x	1.8(9)	9.6(8)	2.5(8)	5.2(8)	5.7(8)		
$n\rho\pi$ to $3\rho\pi$									
4	x	x	x	x	x	x	4.4(9)		
5	x	x	x	x	2.0(8)	5.0(8)	3.4(8)		
C. D_2									
$n\rho\sigma$ to $5\rho\sigma$									
6	x	x	x	x	x	1.5(12)	1.5(12)	1.5(12)	1.5(12)
7	x	x	x	x	2.8(10)	2.7(10)	3.2(10)	3.4(10)	3.7(10)
8	1.8(9)	1.8(9)	1.8(9)	1.6(9)	1.6(9)	1.7(9)	1.5(9)	1.3(9)	1.0(9)

clear vibrational functions of the predissociating state and of the continuum to which predissociation occurs. If the potential curves are similar and the principal quantum numbers of initial and final state are close, the nuclei may make their transition with relatively little change of momentum anywhere in the vibrationally allowed range of R . If the initial and final principal quantum numbers are quite different (and we have in mind a final channel with relatively low n , so that a fair number of vibrational levels may predissociate), then the momentum change of nuclei must be large, the nuclear wave functions of the two states must be rather different, and the rate of predissociation is low because of the cancellations of positive and negative parts of the transition amplitude matrix elements.

Predissociation rates for the cases we have examined are relatively insensitive to the rotational state, in the sense that the rates for highest open channels are always about $5 \times 10^{12} \text{ sec}^{-1}$, are relatively insensitive to vibrational quantum number, and drop rapidly with increasing change in principal quantum number. Typical rates for predissociation of states with rotational quantum numbers $K=8$ and $K=15$ are included in Table VI.

IV. COMPETING DECAY CHANNELS

Vibrationally induced predissociation and autoionization show very different dependencies on principal and vibrational quantum numbers and, to a lesser degree, on the changes in these quantum numbers. For example, total autoionization rates normally increase rapidly, but irregularly, with principal quantum number because, with increasing n , the autoionizing transition can be accomplished with smaller change in vibrational quantum number. This effect tends to override the normal n^{-3} decrease in autoionization rate that occurs for a fixed v and Δv . Measurements of final electron currents, as functions of electron energy, from series of autoionizing states will permit one to sort out the contributions from specific Δv transitions.

To compare autoionization and predissociation and to assess how they compete as decay mechanisms, it is useful to examine the rates of these two processes in several ways. One of these is the conventional rate graph of Fig. 2, which includes some of the autoionizing rates as well as predissociation rates. A second way of summarizing the rate is in terms of a contour plot. In Fig. 3 we show a space in which the abscissa represents the principal quantum number and the ordinate represents the vibrational quantum number. The thresholds for predissociation (to the $5p\sigma$ and $4p\pi$ levels) and for autoionization are shown as shaded bands. Beyond the bands, logarithmically spaced rate contours, with contour intervals corresponding to ten-fold rate changes, indicate how the rates depend on

TABLE VI. Examples of predissociation rates in H_2 , for states of high nuclear angular momentum K . Closed channels are indicated by "x"; "... " indicate that the corresponding bound states do not exist.

n_i	K	v_i	2	3	4	5	6	7	8
6	8	x	x	x	x	x	8.6(7)	5.9(12)	6.2(12)
	18	x	7.6(9)	5.2(12)	4.7(12)
	8	x	x	x	x	5.1(11)	5.6(11)	5.5(11)	...
	18	x	1.5(11)	2.5(11)	2.9(11)
	8	x	x	x	5.7(10)	6.8(10)	7.1(10)	7.0(10)	...
5	18	5.7(9)	1.5(10)	2.0(10)	2.5(10)
	8	x	x	$np\sigma$ to $5p\sigma$	x	x	x	2.4(12)	2.6(12)
6	18	x	x	9.8(11)	1.2(12)
	8	x	x	x	x	1.1(10)	1.1(10)	8.3(9)	8.1(9)
	18	x	4.1(8)	4.1(7)	7.6(7)
7	8	x	x	x	x	2.8(8)	2.8(8)	1.7(8)	6.3(8)
	18	0	2.0(8)	1.5(7)	1.1(4)

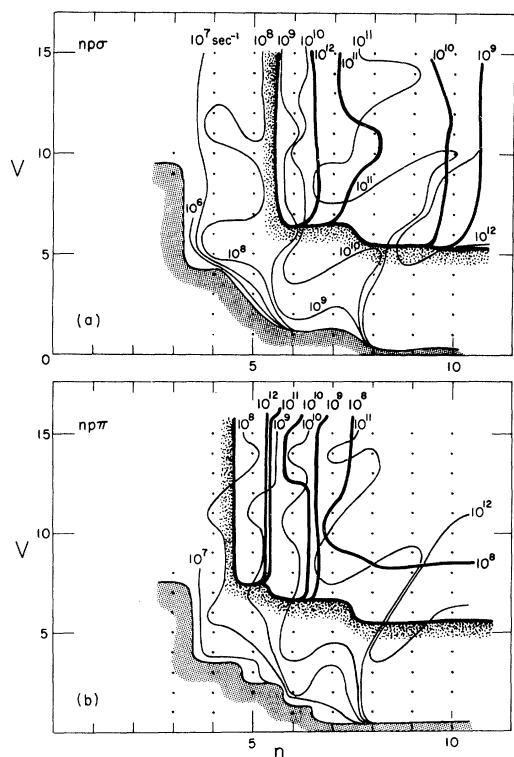


FIG. 3. Contour map for autoionization and predissociation rates. Principal quantum number is plotted on the abscissa and vibrational quantum number on the ordinate. The broad heavily cross-hatched contour represents the threshold for autoionization and the broad stippled contour, the threshold for predissociation, to the $5p\sigma$ from $n(>5)p\sigma$ in the upper diagram and to the $4p\pi$ from $n(>4)p\pi$ in the lower diagram. Autoionization contours are light curves; predissociation contours are heavy and tend to be nearly vertical. Contours represent successive factors of 10 in rates.

n and v . The only physically meaningful parts of the graph are, of course, the points of integral n and v . The contours simply serve to organize the information. Note that the rates of autoionization tend to increase as n and v increase and to define a broad contour rising to a relatively flat plateau at the right, while predissociation rates fall sharply from the threshold ridge toward higher n . Clearly, the two decay processes are competitive whenever contours of equal rates approach each other. In most of the (n, v) space, one set of contours is much higher than the other; we expect, for example, that $6p\sigma$ states with moderately high vibrational quantum numbers will virtually always predissociate rather than autoionize, but that $8p\sigma$ or $9p\sigma$ states with $v = 1, 2$, or 3 will autoionize rather than predissociate.

The competition between autoionization and predissociation is summarized in Fig. 4. Here, the

shaded bands indicate thresholds for minimum values of Δv , for autoionization. Comparison of these bands with the contours in Fig. 3 shows how the Δv propensity rule influences the transition rates. The states indicated by black dots are those decaying primarily by autoionization. States indicated by large circles decay predominantly by predissociation, and states indicated by shaded squares have autoionization and predissociation rates that differ by no more than a factor of 3; i. e., are states for which the two processes are competitive. The assignments of dots, circles, and squares

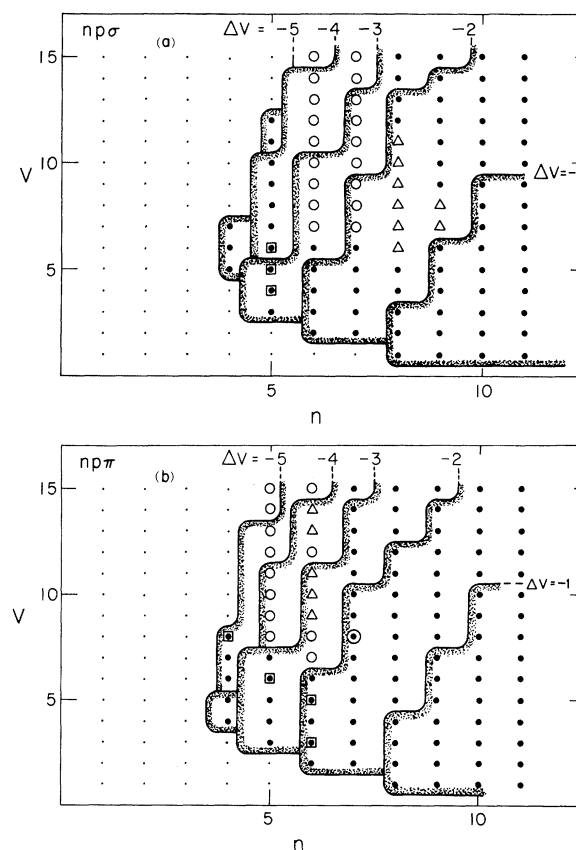


FIG. 4. Qualitative summary plot to illustrate competition between autoionization and predissociation into attractive states. The abscissa represents the principal quantum number and the ordinate, the vibrational quantum number. Contours represent thresholds for transitions of successive values of Δv , the change in vibrational quantum number of the core. Heavy dots represent states decaying primarily by autoionization; open circles indicate states decaying primarily by predissociation, and triangles are used for states for which the two decay processes are competitive (within about a factor of 3). Circumscribed squares or circles are used to indicate states whose decay rates are dominated by second-order coupling; squares indicate that the decay occurs by autoionization and circles by predissociation.

were based on second-order perturbation coupling and the golden rule in order to display the over-all regularities one can expect. Actually, the effects of higher-order coupling are not always negligible. States tied by heavy bars are those for which higher-order coupling contributes significantly to the decay rate of the state whose "normal" lifetimes, based only on second-order perturbation, would be long. The $4p\pi$ states, with $v=6, 7$, and 8 , would normally decay by the very slow $\Delta v = -5$ process. However, by being vibronically coupled to Rydberg states with $n=9$ and 10 , for which $\Delta v = -1$ autoionizing transitions are possible, these low n states can steal a little of the fast autoionizing character of the high n states and should exhibit lifetimes only $\frac{1}{10}$ or even $\frac{1}{100}$ of that based on the direct loss of five vibrational quanta. A similar situation exists, albeit somewhat less dramatically, for "stolen" predissociation. The $7p\pi$, $v=8$ state would autoionize at a rate of $1.0 \times 10^{11} \text{ sec}^{-1}$, but it is vibrationally coupled to the $5p\pi$, $v=10$ state, which predissociates at a rate of $2.7 \times 10^{12} \text{ sec}^{-1}$. The coefficient of $5p\pi$, $v=10$ in $7p\pi$, $v=8$ is -0.383 , which effectively means that the predissociation rate of the perturbed $7p\pi$ is 5×10^{11} , due to its 15% of $5p\pi$, which contributes a rate of $4 \times 10^{11} \text{ sec}^{-1}$. Still another situation arises, at least in principle, when we consider the possibility of *inverse* predissociation coupled to autoionization, via intermediate Rydberg states, or alternatively the reverse of this process - inverse autoionization coupled through intermediate bound states to predissociation. Experimentally, these two processes would appear as associative ionization and dissociative recombination, respectively, possibly with measurable delays. Theoretically such indirect processes must be considered in a treatment of associative ionization and dissociative recombination, along with the direct continuum-continuum coupling processes. For H_2 in thermal systems, the indirect processes play an unimportant role because they require either H_2^+ in a high vibrational state or $\text{H} + \text{H}^*$ with the excited atom in a state that would normally radiate faster than it would make collisions. However, in other systems, in NO for example, such indirect coupling may be significant.⁷

V. ISOTOPE EFFECTS

We have examined the effect of isotopic substitution on both autoionization and predissociation. The gross effect of mass appears in the action of the nuclear momentum operator on the vibrational wave function, especially for transitions with $\Delta v = \pm 1$:

$$\left(\chi_f \left| \frac{\partial \chi_i(v)}{\partial R} \right. \right) \propto (km)^{1/4},$$

where m is the reduced mass of the oscillator, and k is the harmonic force constant. Therefore, the nuclear kinetic-energy matrix element T_1 is proportional to $m^{-3/4}$, and the rates of auto-ionization or predissociation to $m^{-3/2}$.

Going beyond the first approximation, one finds rates for auto-ionization and predissociation as shown in Figs. 5 and 6. Only a few of the curves are displayed in the figure, of course. Note that,

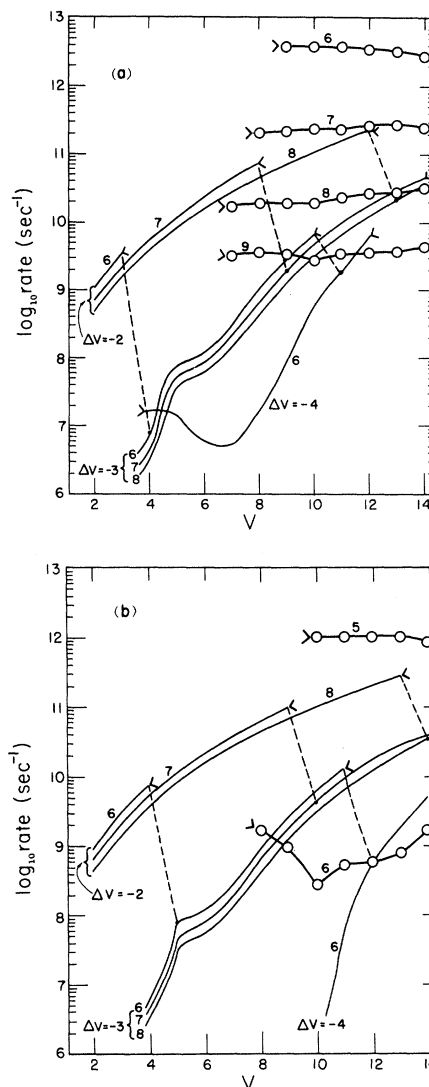


FIG. 5. Autoionization and predissociation rates (sec^{-1}) for HD. (dashed line: autoionization; dash-circle-dash line: predissociation). First and last states for a series of successive initial vibrational states, with fixed n and Δv , are indicated by ">" and "<". Dotted lines connect the end of such a series with the fastest autoionizing point for the next larger value of v . Numbers beside each curve indicate the principal quantum number of the initial excited state.

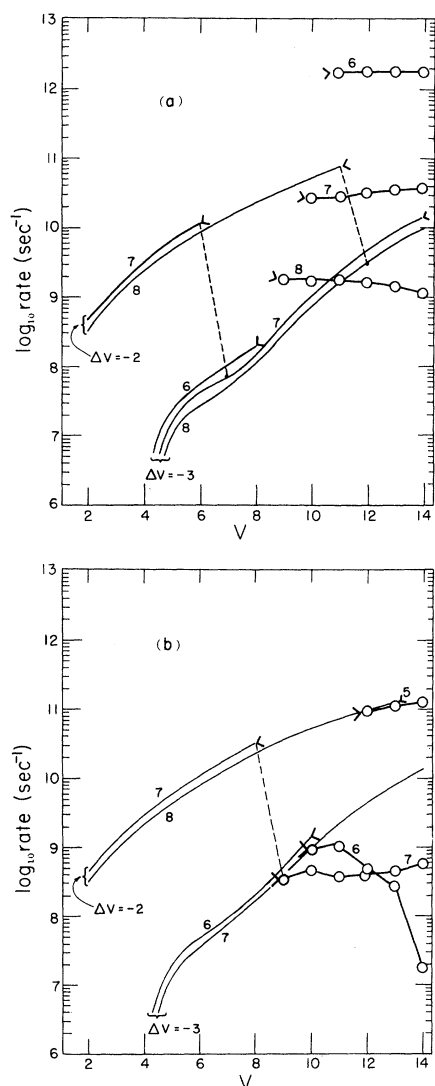


FIG. 6. Autoionization and predissociation rates (sec^{-1}) for D_2 . (dashed line: autoionization; dash-circle-dash line: predissociation). First and last states for a series of successive initial vibrational states, with fixed n and Δv , are indicated by ">" and "<". Dotted lines connect the end of such a series with the fastest autoionizing point for the next larger value of v . Numbers beside each curve indicate the principal quantum number of the initial excited state.

while both processes show straightforward and significant isotope effects, the effect is greatest for the predissociation processes for which $\Delta n \leq -2$, e.g., $7p\sigma \rightarrow 5p\sigma$.

In most cases, the effect of isotopic substitution is merely to lower the rates of both processes. However, in a few situations, the large isotope effect for predissociation, relative to that for autoionization, introduces a very dramatic

change. Note that the $6p\sigma$ states of H_2 , HD, and D_2 decay by predissociation. The $7p\sigma$ of H_2 does the same. For $v \sim 9$ or 10, the two processes are competitive for HD. The $8p\sigma$ of D_2 and the $8p\sigma$ of HD decay by predissociation, wherever both channels are open. Thus, the isotope effect leads to a qualitative change in the decay mechanism, simply because of its different effect in the two decay channels.

We must introduce a warning here about a model-sensitive aspect of our calculations, and at the same time point out one further interesting physical situation which may arise: The availability of a decay channel for some specific bound state depends on the energies of the bound initial and the free final state. For example, in our model, $8p\sigma$ states with $v \leq 3$ can decay, by transfer of one vibrational quantum, in the autoionization channel. If $v > 3$ in this initial electronic state, autoionization can only occur if the core gives up two or more vibrational quanta. That the upper limit of one quantum autoionization for the $8p\sigma$ state occurs at $v=3$ is a consequence of our particular potential model. In real H_2 , the limit comes at a higher quantum number. The same situation occurs in most channels; the $7p\sigma$ of D_2 actually can autoionize via a $\Delta v = -2$ process from quantum states a little higher than the $v=6$ state, which is the upper limit for this process in our model.

Let us examine the $6p\sigma$ and $7p\sigma$ states of D_2 . Figure 6 shows the curves for the $7p\sigma$, for both $\Delta v = -2$ and $\Delta v = -3$ rates, with the upper limit for $\Delta v = -2$ at $v=6$. For $v=7$, the autoionization rate is about 5×10^7 . For the $6p\sigma$ state, autoionization is only possible via loss of three vibrational quanta from the H_2^+ core, from the states $v=3$ through $v=8$. The processes are slow; their rates increase from 7×10^6 to 2×10^8 , as v increases. Autoionization of the $6p\sigma$ state of D_2 in the vibrational states $v=3$ and $v=4$ is actually slower than the radiation rate of circa $2 \times 10^7 \text{ sec}^{-1}$. For the $7p\sigma$, in our model, the nonradiative decay processes of autoionization and predissociation are much faster than radiation, except in the one channel $v=7$, where autoionization at a rate of $7 \times 10^7 \text{ sec}^{-1}$ is probably only faster than radiation by about a factor of 4 or 5. The implications of these results of the model calculation are that we may expect to see some real situations in which an excited diatomic molecule exhibits autoionization of the low vibrational states of a specific electronic state, predissociation from high vibrational states of the same electronic state, and occasionally, radiative decay only from intermediate vibrational levels. Whether this actually occurs in D_2 remains to be studied.

ACKNOWLEDGMENTS

This work was supported in part by Grant No.

GP-5535 from the National Science Foundation. Some of the computations were performed at Northern Europe University Computing Center, Lyngby, Denmark; we are indebted to this Center

for providing us with computer time and facilities. Part of the work was carried out at the Aspen Center for Physics, for whose services we are indebted.

¹R. S. Berry and S. E. Nielsen, preceding paper Phys. Rev. A 1, 383 (1970).

²S. E. Nielsen and R. S. Berry, Chem. Phys. Letters 2, 503 (1968).

³W. A. Chupka and J. Berkowitz, J. Chem. Phys. 48, 5726 (1968).

⁴W. A. Chupka and J. Berkowitz, J. Chem. Phys. (to

be published).

⁵F. J. Comes and H. O. Wellern, Z. Naturforsch. 23a, 881 (1968).

⁶R. S. Berry, J. Chem. Phys. 45, 1228 (1966).

⁷J. N. Bardsley, Chem. Phys. Letters 1, 229 (1967).

⁸A. Russek, M. R. Patterson, and R. L. Becker, Phys. Rev. 167, 17 (1968).

PHYSICAL REVIEW A

VOLUME 1, NUMBER 2

FEBRUARY 1970

Mechanism of Ultrasonic Cavitation Nucleation in Liquid Helium by Quantized Vortices*

P. M. McConnell,[†] M. L. Chu, Jr.,[‡] and R. D. Finch

University of Houston, Houston, Texas 77004

(Received 7 July 1969)

The interaction between an ultrasonic field and one or a few quantized vortex lines in He II was investigated using the audible cavitation threshold as a means of detection. Experiments involved both rotating ultrasonic buckets and two shafts, each with a paddle attached, rotatable in the same or opposite sense near an ultrasonic field. Histograms of cavitation threshold measurements were not Gaussian, but appeared to be bimodal. The high threshold mode was most frequent in the quiescent state, but the lower mode was most frequent with rotation. The threshold values were found to fluctuate with time both with and without rotation. Slight and gradual reductions of audible threshold were observed in the rotating bucket sometimes, beginning at speeds less than that predicted by the Arkhipov-Vinen formula. Reductions at speeds higher than the Arkhipov-Vinen value were not directly proportional to the total number of vortices believed to be present in the bucket. Two shafts with paddles rotating in opposite senses caused larger reductions in threshold than a single shaft and paddle; but this was not the case when the shafts rotated in the same sense.

I. INTRODUCTION

Of the possible sources of cavitation nuclei (stabilized pockets of undissolved gas or vapor, cosmic rays or radioactivity, and free vortices), the most plausible one for He II is the vortex.¹⁻⁴ Finch and Chu² found that rotation of a shaft with an attached paddle above a critical speed near an ultrasonic field lowered the audible threshold of He II. This critical speed corresponded to that required for quantized circulation around the shaft, i. e.,

$$\omega_c = \hbar/ma^2, \quad (1)$$

where a is the shaft radius. It was concluded that a single free-vortex "tail" migrated into the sound field giving rise to the threshold reduction. An alternative suggestion by Hsieh⁵ was that ring vortices peel off the end of the shaft and penetrate into the sound field.

Using Dean's⁶ free-vortex model, Finch and Chu² pointed out that the tension required to rupture a singly quantized vortex core was not much less than that needed to break the molecular bonds. Thus, it was difficult to understand how a single core could act as the cavitation nucleus, and the nature of the vortex-ultrasound interaction remained in question. Recently, the suggestion has been made